Rapid Communications

Origin of anomalous polymer-induced fluid displacement in porous media

Shima Parsa
John A. Paulson School of Engineering and Applied Sciences, Harvard University, Cambridge, Massachusetts 02138, USA
and School of Physics and Astronomy, Rochester Institute of Technology, Rochester, New York 14623, USA

Enric Santanach-Carreras
Total SA, Pôle dEtudes et Recherche de Lacq, BP 47, 64170 Lacq, France
and Laboratoire Physico-Chimie des Interfaces Complexes, Total SA-ESPCI-CNRS, Route Départementale 817, 64170 Lacq, France

Lizhi Xiao
State Key Laboratory of Petroleum Resources and Prospecting, China University of Petroleum, Beijing 102249, China
and Harvard SEAS-CUPB Joint Laboratory on Petroleum Science, Cambridge, Massachusetts 02138, USA

David A. Weitz*
John A. Paulson School of Engineering and Applied Sciences, Harvard University, Cambridge, Massachusetts 02138, USA;
Department of Physics, Harvard University, Cambridge, Massachusetts 02138, USA;
and Wyss Institute for Biologically Inspired Engineering at Harvard University, Boston, Massachusetts 02115, USA

(Received 16 May 2019; accepted 8 January 2020; published 3 February 2020)

Immiscible displacement of fluids with large viscosity mismatch is inherently unstable due to viscous fingering, even in porous media where capillary forces dominate. Adding polymer to the displacing fluid reduces the viscosity mismatch and suppresses the viscous fingering instability thereby increasing the fluid displacement leading to extensive use in applications such as oil recovery. Surprisingly, however, an increase in displacement occurs even for very large viscosity mismatches. Moreover, significant additional displacement is observed when the polymer solution is followed by additional water flow. Thus, the fundamental physics of this phenomenon remains unclear. To understand this behavior, we use confocal microscopy to visualize the displacement of oil in a three-dimensional micromodel of a porous medium and simultaneously measure the local flow velocities of the displacing fluid. We find that the increased displacement results from a counterintuitive effect: polymer retention in the medium and the resultant local changes in flow. Typically retention is avoided since it reduces the permeability of the medium; instead, we find that large and heterogeneous local changes in flow lead to sufficiently large enough viscous forces at the interface of the immiscible fluids resulting in increased displacement.

DOI: 10.1103/PhysRevFluids.5.022001

*weitz@seas.harvard.edu

I. INTRODUCTION

Fluid-fluid displacement occurs in many environmental and industrial settings ranging from drying of wood to oil recovery [1–4]. When a less viscous fluid displaces a more viscous fluid, the interface becomes unstable and viscous fingering occurs. This behavior is widely studied in simple geometries, such as in a narrow gap between two parallel plates, where it is known as the Saffman-Taylor instability [5]. Viscous fingering also occurs when a low-viscosity fluid displaces a high-viscosity fluid in porous media; however, here, capillary forces at the interfaces within the medium are essential and the physics of the instability is less well understood [6–8]. Nevertheless, understanding the underlying physics in immiscible displacement in porous media is crucially important for many applications. One of the most important is oil recovery: Viscous fingering, combined with the intrinsic heterogeneities of porous reservoir rocks, leads to inefficient sweep and poor recovery when oil is displaced by water flooding [9], which is invariably the first means of extended oil recovery. As a result, a large fraction of oil, up to 75%, remains trapped in the reservoir. One way to access this large amount of residual oil is to reduce the viscosity mismatch between oil and water. This concept has led to the development of polymer flooding, one of the more economically viable methods of further enhancing oil recovery. A small concentration of polymer is added to the water to increase its viscosity, which should mitigate the viscous-fingering instability, leading to an improved sweep of the oil and increasing recovery by as much as 20% of the original oil in the reservoir [4,10–14]. However, the physics of this effect is not well understood: Enhanced recovery is seen even for very viscous oils, when the viscosity mismatch remains highly unfavorable [12,13,15–18]. Moreover, most of the additional oil is not recovered upon injection of the relatively small amount of polymer solution but is instead recovered during the subsequent water flow, known as the chase water. Surprisingly, bulk transport measurements suggest that the average viscous forces exerted by both the polymer solution and the chase water are much smaller than the capillary force that traps the oil and thus should not displace it [4]. Hence, our understanding of the underlying physics of this phenomenon is severely lacking, yet is essential for its further development and improvement, which is crucial given the limitation of natural resources and the cost and difficulty of finding new reserves.

Here, we use pore level measurements to determine the underlying physical mechanism that leads to the additional displacement of viscous oil in a porous medium by a polymer solution. We use confocal microscopy to measure the pore-scale velocities of the displacing fluid in a three-dimensional micromodel; we also measure the bulk transport properties of the fluids in the medium. We show that retention of polymer causes a reduction of the medium permeability. The resultant recovery cannot be accounted for by the higher average pressure due to changes in permeability. However, the pore-scale measurements show this local reduction in permeability leads to highly heterogeneous changes in the local flow velocities which results in locally large additional viscous forces by the displacing fluid; these overcome the capillary force and mobilize oil. These results provide direct evidence for the physical mechanism that leads to the surprising enhanced recovery of viscous oil by both the polymer flow and the subsequent chase water.

II. EXPERIMENTAL METHODS

We investigate the pore level dynamics of oil displaced by a polymer solution using a three-dimensional (3D) micromodel which allows direct observation of the fluids using optical microscopy. We prepare a rigid micromodel by sintering a random loose packing of monodisperse borosilicate glass beads with radius of $R = 19\ \mu$m in a square quartz capillary [19]. The cross-sectional area and length of the medium are $A = 9\ \text{mm}^2$ and $L = 4$ cm, respectively, as seen in the schematic in Fig. 1(a). The porosity of the medium is $\phi = 45 \pm 3\%$. To directly observe the fluids in the medium by confocal microscopy, we formulate a displacing fluid, 86 wt % dimethyl sulfoxide and 14 wt % water, to match the index of refraction of the glass beads, $n = 1.465$. To investigate immiscible displacement for fluids with a very large viscosity mismatch a mixture of 85 wt % heavy crude oil and 15 wt % dodecane is used for the oil phase. The viscosity of the

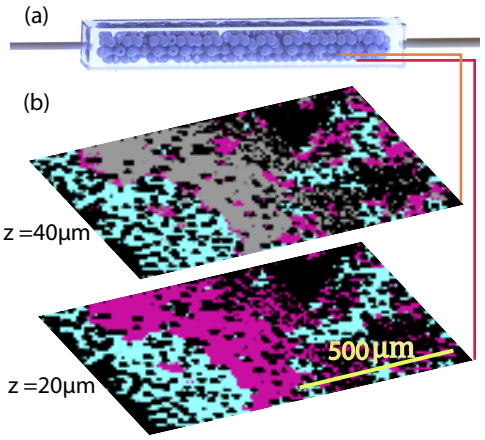

FIG. 1. Imaging the 3D micromodel. (a) Schematic of the 3D micromodel. (b) Two optical slices in z direction at depths of 20 and 40 μm. The medium is filled with both the displacing fluid (blue) and crude oil (purple). Gray represents the typical shadow of crude oil. Any areas without fluorescent signal, glass beads, and shadow of crude oil, are black.

oil mixture, $\mu_{\text{oil}} = 2.4$ Pa s, matches that of the crude oil at the pressure and temperature of the reservoir and is much larger than that of the displacing fluid, $\mu_{df} = 2.8$ mPa. We use a long chain linear polymer, partially hydrolyzed polyacrylamide, with molecular weight of $M_w = 20$ MDa. This commercial grade polymer, known as Flopaam 3630S, is commonly used in oil recovery. The polymer is dissolved in deionized water with salt, NaCl, at 0.35 g/l. The polymer concentration is 0.25 g/l, larger than the overlap concentration, $c^* = 0.2$ g/l. The polymer solution is slightly shear thinning with a zero-shear rate viscosity of $\mu_{p,0} = 27$ mPa s (see Supplemental Material [20] for the measured viscosities).

The configurations of oil and displacing fluid in the medium are monitored using confocal microscopy. We acquire 3D stacks of confocal micrographs at 10 μm intervals in the z direction. The two fluids are distinguished using two separate fluorescent wavelengths: asphaltenes naturally present in crude oil autofluoresce and we add 0.01 vol % fluorescein sodium salt to the displacing fluid. The solid matrix appears dark in the images. We denote the oil using purple and the displacing fluid using blue in a typical confocal image plane 20 μm into the sample, shown in Fig. 1(b). Since crude oil is not transparent, it obstructs the light and prevents it from reaching any image planes above; thus, the image 40 μm into the sample still reveals some oil and water but a large region is obstructed by the oil below, as shown in gray in Fig. 1(b). Nevertheless, we are still able to image to a depth of about 200 μm. To determine the exact amount of displaced oil, the effluent is collected and dissolved in tetrahydrofuran, a good solvent for both phases. We then measure the light absorption with a UV-vis spectrometer to determine the concentration of oil in the effluent (see Supplemental Material [20] for measured absorption of light at different oil concentrations).

To investigate the nature of the displacement of viscous oils by polymer solution, we mimic the polymer flooding for oil recovery using our 3D micromodel. This is accomplished by first flowing the displacing fluid into the fully oil-saturated medium at a flow rate of $Q = 100$ l/h corresponding to a Darcy velocity, Q/A, of $v = 3$ μm/s. The resultant capillary number, the relative strength of the viscous force of the displacing fluid to the capillary force that traps the oil, $\text{Ca} = (\mu_{df} v)/\gamma$, is 2×10^{-7}. Here, the interfacial tension between oil and the displacing fluid is $\gamma = 20$ mN/m. The initial water flow is well within the capillary regime where capillary forces dominate as shown in similar but independent experiments, where small changes in velocity of the displacing fluid do not affect the recovery [21,22]. We continue with an extended flow of the displacing fluid until no additional oil is produced, allowing us to distinguish any further recovery from that of the initial water flow. We find that 23% of the oil in the medium is recovered after the initial water flow.

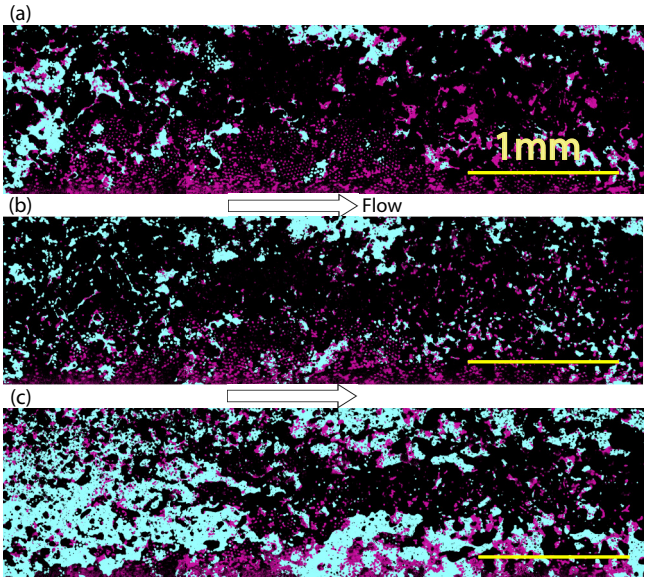

FIG. 2. Configuration of crude oil (purple) and displacing fluid (blue) in the medium during polymer flooding after (a) initial water flow, (b) polymer flow, and (c) chase water. The images represent one optical slice which is at the same z depth as the inlet on the left and as the outlet on the right side of the image.

We next investigate the effect of polymer flooding on the configuration of trapped oil in the medium. We first prepare the medium by flowing 2 pore volumes of deionized water into the medium. This additional wash avoids precipitation of the polymer in the displacing fluid, which is a poor solvent for the polymer. To ensure that no additional viscous force is exerted on the trapped oil, the wash is at a slightly smaller $\mathrm{Ca} = 8 \times 10^{-8}$. We then flow 5 pore volumes of the polymer solution through the medium at the same Ca as that of the initial water flow. No additional oil is observed in the effluent during this polymer flow. To mimic the full behavior of polymer flow in an oil reservoir, an additional flow of the displacing fluid, known as chase water, follows the polymer flooding. The chase water, here, consists of a wash of 2 pore volumes of deionized water at the lower Ca. This is followed by 15 pore volumes of the displacing fluid at the same Ca as that of the initial water flow. Surprisingly, a significant additional amount of oil, 17%, is recovered during the flow of chase water, even though none is recovered during the polymer flow. Interestingly, chase water displaces oil even though it is at the same capillary number as the initial water flow.

To help understand these results, we compare the confocal images after the chase water with those after the initial water flow and with those after the polymer flow. After the polymer flow, only a small amount of additional oil is displaced as compared to that after the initial water flow, as can be seen by comparing the amount of displacing fluid, identified by the blue regions, in Figs. 2(a) and 2(b). By contrast, the chase water displaces much more oil from the medium, as shown by the larger regions of blue in Fig. 2(c). Here, we only account for the amount of recovered oil in the areas where light is not obstructed by oil in the lower planes and the fluorescent displacing fluid is identified. The areas blocked by the shadow of crude oil do not contribute to this measurement. However, the measured amount of displaced oil from confocal micrographs is consistent with the exact amount of recovered oil, which is determined by measuring the concentration of oil in effluent.

III. RESULTS AND DISCUSSION

The observation of oil displacement only during the chase water, but not during the polymer flow, suggests that some polymer may be retained in the medium. This would directly affect the

medium permeability. To test this possibility, we monitor the permeability in a similar, but separately prepared, micromodel filled only with water. We measure the pressure drop, ΔP, across the medium at constant flow rate and determine the permeability using Darcy's law, $k = \mu_w \frac{QL}{A} \Delta P$, where $\mu_w = 9 \times 10^{-4}$ Pa s is the viscosity of water. The permeability is 5×10^{-12} m^2; it decreases significantly, by 30%, upon flow of 5 pore volumes of the polymer solution, confirming the retention of polymer. The reduction in permeability of the medium after polymer flow is in agreement with the observation of a decrease in the permeability of a single glass capillary tube with a radius of 50 μm, after flow of a similar polymer solution [23,24].

Does the permeability reduction lead to displacement of oil? Reduction in permeability, at a constant flow rate, can lead to an increase in the effective capillary number; hence, additional displacement of oil is possible. To test this, we use a mean-field description to determine the viscous pressure drop in the medium and compare it with the capillary pressure that traps the residual oil. Using Darcy's law, the mean-field viscous pressure drop, ΔP_v, across an oil ganglion of length L_{oil} is $\Delta P_v = (\mu_{df} v)/(k_{df} k) L_{\text{oil}}$, where k_{df} is the relative permeability for the displacing fluid. The medium permeability, $k_{df} k$, is 1.2×10^{-13} m^2, due to the presence of trapped oil and retention of polymer. The value for the permeability of the medium is extrapolated from direct measurement of the relative permeability of the medium in similar experiments (see Supplemental Material [20] for reference). The length of the largest oil ganglion displaced by the chase water is $L_{\text{oil}} = 3$ mm, determined by comparing the configuration of oil after the initial water flow [Fig. 2(a)] with that after the chase water [Fig. 2(c)]. The viscous pressure across this oil ganglion after the reduction in permeability due to the polymer flow, is $\Delta P_v = 70$ Pa. By contrast, the capillary pressure of the oil ganglion, $P_{\text{ca}} = 2\gamma \cos\theta / r$, is approximately 1000 Pa, assuming that it is trapped by the average pore entrance of $r = 3$ μm estimated for a random packing of these beads [25,26]. The contact angle between oil and displacing fluid on the surface of glass is $\theta = 60^\circ$ and does not change after polymer retention (see Supplemental Material [20] for the measurements). Therefore, even with the increase due to the permeability reduction, the average viscous pressure is still much smaller than the capillary pressure that traps oil. Thus, changes in permeability do not account for the additional recovery consistent with previous results [14].

The mean-field description of flow in porous media ignores an essential feature of the behavior: the complex network of pores in the medium results in a highly heterogeneous spatial distribution of the flow [27–31], which is significantly exacerbated by the residual oil [32]. To explore the consequence of this heterogeneity, we probe the dynamics of the displacing fluid at pore level and around trapped oil using confocal microscopy. For these measurements, however, a fully transparent system is needed; thus, the crude oil is replaced with a model oil, Cargille immersion oil with the same index of refraction as the glass. We add a surfactant, Tween 20, at 0.1% by weight to change the affinity of the oil to the glass to ensure sufficient residual oil after water flow. The interfacial tension between the model oil and the displacing fluid is 15 mN/m and the viscosity of the model oil is 12 mPa s. We repeat the polymer flow experiments using these fluids. The initial water flow to displace model oil from the medium is carried out at $v = 3$ μm/s, resulting in $\text{Ca} = 7 \times 10^{-7}$. We directly image the trapped oil in the medium after the initial water flow using confocal microscopy. The displacing fluid is replaced by water at smaller $\text{Ca} = 1.5 \times 10^{-7}$ similar to the wash for crude oil. This is followed by 5 pore volumes of the polymer solution at the same Ca as the initial water flow, and then a second water wash at the lower Ca to remove any remaining polymer. We image the configuration of trapped oil by flowing one pore volume of the displacing fluid at low $\text{Ca} = 2 \times 10^{-7}$, ensuring no disruption of oil. This is followed by the chase fluid, which consists of 12 pore volumes of the displacing fluid at the same higher Ca as used for the initial water flow. The configuration of a typical oil ganglion is observed with the confocal microscope. Its shape is unchanged by the polymer flow as seen by comparing the highlighted area in the image after the water flow with that after the polymer flow in Figs. 3(a) and 3(b). By contrast, the oil ganglion is completely displaced after the chase water as seen in Fig. 3(c). While no additional oil is displaced during the polymer flow, an additional 9% of the original oil is recovered during the chase water; this is 50% of the oil remaining in the medium after the initial water flow.

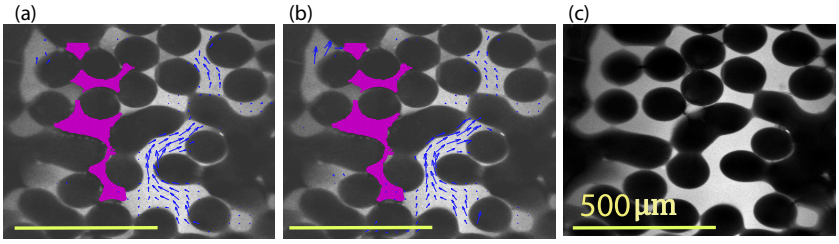

FIG. 3. Configuration of a ganglion of model oil (purple) trapped in 3D micromodel along with the measured velocities of displacing fluid in blue. The flow is observed (a) immediately after the initial water flow, (b) immediately after the polymer flow, and (c) after chase water where the oil ganglion is removed.

To quantify the effect of the polymer flow on the pore level dynamics of the displacing fluid, we add additional steps to the experiment to measure the fluid velocities both before and after the polymer flow. We replace the displacing fluid with one that is seeded with 1 μm diameter fluorescent tracer particles at 0.005 vol % and use particle tracking velocimetry to measure the velocity around each oil ganglion [33]. The possibility of accumulation of tracer particles in small pores and clogging is significantly reduced by using a micromodel made with larger glass beads, $R = 75$ μm.

The average velocity in all the pores increases by almost 50% compared to that before the polymer flow, consistent with the expectation due to the reduction in permeability. To determine if the changes in velocity are sufficient to mobilize the oil, we compare the viscous pressure after the polymer flow with the capillary pressure that traps an oil ganglion that is displaced by the chase water shown in Fig. 3. The capillary pressure for this oil ganglion is $P_{\mathrm{ca}} = 280$ Pa, as determined by directly measuring its curvature and length, $L_{\mathrm{oil}} = 800$ μm (see Supplemental Material [20] for the 3D reconstruction of this oil ganglion). Using the Darcy approximation and the measured average velocity, we estimate the average viscous pressure across this oil ganglion after the polymer flow to be $\Delta P_v = 12$ Pa. This is much smaller than the capillary pressure. Therefore, the average increase in velocity of the displacing fluid is insufficient to account for the displacement of oil. However, the local changes in the velocities following the polymer flow are very heterogeneous and, in some pores, can be as much as eight times larger, as seen, for example, by comparing the sizes of the arrows in the pore in the upper left corner of Figs. 3(a) and 3(b). We therefore explicitly measure the viscous stress on the surface of the oil ganglion using the fully resolved velocities of the displacing fluid around oil but restricted to the two-dimensionalization (2D) visualization plane. At the interface of the two fluids the normal component of the viscous stress is balanced by the capillary pressure [34]. The total viscous force exerted by the displacing fluid on the oil, is equal to the sum of the local forces over the entire surface of the ganglion.

$$\vec{F} = \oint \tau_{ij}\, dA_j. \tag{1}$$

Here, $\tau_{ij} = \mu_{df}[(du_i)/(dx_j)]$ is the normal component of the viscous stress tensor. We determine the viscous stress from the measured values of the maximum velocities of the displacing fluid in direct contact with oil and the dimensions of the pore. The viscous pressure is determined numerically by summing the force over the discrete area of the interface of the oil ganglion in contact with the displacing fluid. Remarkably, $\Delta P_v = 145$ Pa, which is almost equal to the capillary pressure at the interface of oil and displacing fluid. Thus, only when the local heterogeneities of the velocity field of the displacing fluid are included is the viscous pressure sufficiently large to mobilize the oil. Moreover, the local viscous pressure after the polymer flow is three times larger than that before the polymer flow. The 2D velocity measurement gives a good estimate of the viscous pressure; however, the exact value can only be determined from a full 3D velocity field around the ganglion, which is not available in this experiment. Another way to estimate the viscous pressure

is to reduce the complex geometry of the medium around the trapped oil into a tube carrying the displacing fluid. The length of the tube is equal to the length of the oil ganglion, and its diameter is equal to that of the pore in contact with the oil with the largest velocity of displacing fluid. We calculate the viscous pressure assuming Poiseuille flow in this tube (see Supplemental Material [20] for more details). We obtain a value nearly identical to our first estimate; moreover, this value is nearly an order of magnitude larger than the value determined before the polymer flow. This further highlights the significant difference between the local flow velocity and the average value. Similar behavior is measured for other ganglia observed to be displaced by the chase water. Similar heterogeneity will occur in the system with crude oil; this will lead to local viscous pressure drops that are sufficient to displace the residual crude oil, consistent with our observations.

IV. CONCLUSIONS

These results are in sharp contrast with the commonly accepted mechanism for displacement of oil by polymer flow. The improved displacement is generally believed to be due to the suppression of viscous fingering instabilities at the interface of the two fluids due to the increased viscosity of the displacing fluid due to the polymer. However, this is not the case in our measurements: Although the polymer solution has a higher viscosity than water, it is still two orders of magnitude smaller than the oil. Moreover, no additional recovery is observed during polymer flow. Another proposed mechanism for recovery by polymer flow is fluctuations in the viscous pressure due to the non-Newtonian behavior of the polymer solution, known as elastic turbulence [35–39]. However, no oil is displaced during the polymer flow but is instead only displaced during the chase water; thus, this mechanism cannot be responsible for the additional displacement of oil. This is further corroborated by independent measurements of the velocities of the polymer solution in the micromodel in the absence of oil: Velocity fluctuations are first observed only at flow rates at least an order of magnitude larger than those used here (see Supplemental Material [20] for demonstration of the flow fluctuations at high flow rates). Another general belief is that fluid displacement is always improved with increased permeability since fluids experience less resistance. Surprisingly, polymer retention reduces the permeability yet still enhances recovery. However, the permeability reduction itself is not sufficient to displace additional oil, even at constant volumetric flow rate. Instead, the highly heterogeneous nature of the local changes in fluid velocity after the polymer flow lead to large fluctuations in velocities which are essential for polymer-enhanced oil recovery.

Our findings provide a physical understanding of the pore level effects of polymer flow that leads to enhanced recovery. These results demonstrate that flow of polymer can lead to mobilization of oil at concentrations much smaller than that needed to increase the viscosity of the polymer solution to match that of the oil. Moreover, micromodel measurements provide detailed information on the local dynamics of fluids not readily accessible through other imaging techniques used for rock samples. Furthermore, local flow dynamics can be probed in carefully prepared micromodels with a wide range of pore sizes and wettability to study the behavior of different polymers and different crude oils.

ACKNOWLEDGMENTS

It is a pleasure to acknowledge S. S. Datta and S. Berg for stimulating discussion. This work was supported by the National Science Foundation (DMR-1708729), Harvard NSF MRSEC (DMR-1420570), Total E&P Recherche Developpement Awards No. FR00006025 and No. FR00006847, and China University of Petroleum, Beijing China 111 project (B13010).

[1] S. Whitaker, Simultaneous heat, mass, and momentum transfer in porous media: A theory of drying, Adv. Heat Transfer **13**, 119 (1977).

[2] M. Sahimi, *Flow and Transport in Porous Media and Fractured Rock: From Classical Methods to Modern Approaches* (Wiley-VCH Verlag GmbH Co., Weinheim, 2011).
[3] J. Bear, *Dynamics of Fluids in Porous Media* (Dover, New York, 1988).
[4] K. S. Sorbie, *Polymer-Improved Oil Recovery* (CRC Pr I Llc, 1991).
[5] P. G. Saffman and G. Taylor, The penetration of a fluid into a porous medium or Hele-Shaw cell containing a more viscous liquid, Proc. R. Soc. London, Ser. A **245**, 312 (1958).
[6] J. P. Stokes, D. A. Weitz, J. P Gollub, A. Dougherty, M. O. Robbins, P. M. Chaikin, and H. M. Lindsay, Interfacial Stability of Immiscible Displacement in a Porous-Medium, Phys. Rev. Lett. **57**, 1718 (1986).
[7] B. Zhao, C. W. MacMinn, and R. Juanes, Wettability control on multiphase flow in patterned microfluidics, Proc. Natl. Acad. Sci. USA **113**, 10251 (2016).
[8] D. Rabbani, H. S. Or, Y. Liu, C-Y. Lai, N. B. Lu, S. S. Datta, H. A. Stone, and N. Shokri, Suppressing viscous fingering in structured porous media, Proc. Natl. Acad. Sci. USA **115**, 4833 (2018).
[9] R. Lenormand and C. Zarcone, Invasion Percolation in an Etched Network—Measurement of a Fractal Dimension, Phys. Rev. Lett. **54**, 2226 (1985).
[10] S. Thomas, Enhanced oil recovery—An overview, Oil Gas Sci. Technol. **63**, 9 (2008).
[11] B. Rossen, L. W. Lake, R. Johns, and G. Pope, *Fundamentals of Enhanced Oil Recovery* (Society of Petroleum Engineers, 2014).
[12] D. Levitt, M. Bourrel, I. Bondino, S. Jouenne, and J.-P. Gingras, The interpretation of polymer coreflood results for heavy oil, Society of Petroleum Engineers (2011), doi: 10.2118/150566-MS.
[13] C. Huh and G. Pope, Residual oil saturation from polymer floods: Laboratory measurements and theoretical interpretation, Society of Petroleum Engineers (2008), doi: 10.2118/113417-MS.
[14] P. Barreau, D. Lasseux, H. Bertin, P. Glenat, and A. Zaitoun, An experimental and numerical study of polymer action on relative permeability and capillary pressure, Pet. Geosci. **5**, 201 (1999).
[15] D. Levitt, S. Jouenne, I. Bondino, E. Santanach-Carreras, and M. Bourrel, Polymer flooding of heavy oil under adverse mobility conditions, Society of Petroleum Engineers (2013), doi: 10.2118/165267-MS.
[16] E. Delamaide, A. Zaitoun, G. Renard, and R. Tabary, Pelican Lake field: First successful application of polymer flooding in a heavy oil reservoir, Society of Petroleum Engineers (2013), doi: 10.2118/165234-MS.
[17] D. Wang, Y. Hao, E. Delamaide, Z. Ye, S. Ha, and X. Jiang, Results of two polymer flooding pilots in the central area of Daqing oil field, Society of Petroleum Engineers (1993), doi: 10.2118/26401-MS.
[18] D. Wang, R. S. Seright, Z. Shao, and J. Wang, Key aspects of project design for polymer flooding at the Daqing oilfield, Society of Petroleum Engineers **11**, 1117 (2008), doi: 10.2118/109682-PA.
[19] A. T. Krummel, S. S. Datta, S. Munster, and D. A. Weitz, Visualizing multiphase flow and trapped fluid configurations in a model three-dimensional porous medium, AIChE J. **59**, 1022 (2013).
[20] See Supplemental Material at http://link.aps.org/supplemental/10.1103/PhysRevFluids.5.022001 for additional experimental measurements and analysis.
[21] N. R. Morrow, I. Chatzis, and J. J. Taber, Entrapment and mobilization of residual oil in bead packs, Society of Petroleum Engineers **3**, 927 (1988), doi: 10.2118/14423-PA.
[22] S. S. Datta, T. S. Ramakrishnan, and D. A. Weitz, Mobilization of a trapped non-wetting fluid from a three-dimensional porous medium, Phys. Fluids **26**, 022002 (2014).
[23] P. L. J. Zitha, G. Chauveteau, and L. Leger, Unsteady-state flow of flexible polymers in porous media, J. Colloid Interface Sci. **234**, 269 (2001).
[24] C. A. Grattoni, P. F. Luckham, X. D. Jing, L. Norman, and R. W. Zimmerman, Polymers as relative permeability modifiers: Adsorption and the dynamic formation of thick polyacrylamide layers, J. Pet. Sci. Eng. **45**, 233 (2004).
[25] M. Yanuka, F. A. L. Dullien, and D. E. Elrick, Percolation processes and porous media, J. Colloid Interface Sci. **112**, 24 (1986).
[26] G. Mason and N. Morrow, Menisucus displacement curvatures of a perfectly wetting liquid in capillary pore throats formed by spheres, J. Colloid Interface Sci. **109**, 46 (1986).
[27] A. Cortis, Y. J. Chen, H. Scher, and B. Berkowitz, Quantitative characterization of pore-scale disorder effects on transport "inhomogeneous" granular media, Phys. Rev. E **70**, 041108 (2004).

[28] T. Le Borgne, M. Dentz, and E. Villermaux, Stretching, Coalescence, and Mixing in Porous Media, Phys. Rev. Lett. **110**, 204501 (2013).
[29] P. K. Kang, J. P. de Anna, P. Nunes, M. J. Bijeljic, B. Blunt, and R. Juanes, Pore-scale intermittent velocity structure underpinning anomalous transport through 3-D porous media, Geophys. Res. Lett. **41**, 6184 (2014).
[30] K. Alim, S. Parsa, D. A. Weitz, and M. P. Brenner, Local Pore Size Correlations Determine Flow Distributions in Porous Media, Phys. Rev. Lett. **119**, 144501 (2017).
[31] V. L. Morales, M. Dentz, M. Willmann, and M. Holzner, Stochastic dynamics of intermittent pore-scale particle motion in three-dimensional porous media: Experiments and theory, Geophys. Res. Lett. **44**, 9361 (2017).
[32] S. S. Datta, H. Chiang, T. S. Ramakrishnan, and D. A. Weitz, Spatial Fluctuations of Fluid Velocities in Flow through a Three-Dimensional Porous Medium, Phys. Rev. Lett. **111**, 064501 (2013).
[33] S. Parsa, J. S. Guasto, M. Kishore, N. T. Ouellette, J. P. Gollub, and G. A. Voth, Rotation and alignment of rods in two-dimensional chaotic flow, Phys. Fluids **23**, 043302 (2011).
[34] W. M. Deen, *Analysis of Transport Phenomena*, 2nd ed. (Oxford University Press, New York, 1998).
[35] A. F. Morais, H. Seybold, H. J. Herrmann, and J. S. Andrade, Jr., Non-Newtonian Fluid Flow through Three-Dimensional Disordered Porous Media, Phys. Rev. Lett. **103**, 194502 (2009).
[36] T. Sochi, Flow of non-Newtonian fluids in porous media, J. Polym. Sci., Part B: Polym. Phys. **48**, 2437 (2010).
[37] P. Qi, D. H. Ehrenfried, H. Koh, and M. T. Balhoff, Reduction of residual oil saturation in sandstone cores by use of viscoelastic polymers, Society of Petroleum Engineers **22**, 447 (2017).
[38] J. Mitchell, K. Lyons, A. M. Howe, and A. Clarke, Viscoelastic polymer flows and elastic turbulence in three-dimensional porous structures, Soft Matter **12**, 460 (2016).
[39] A. Clarke, A. M. Howe, J. Mitchell, J. Staniland, and L. A. Hawkes, How viscoelastic polymer flooding enhances displacement efficiency, Society of Petroleum Engineers (2015), doi: 10.2118/174654-MS.